CHALMERS
UNIVERSITY OF TECHNOLOGY

An Exploration of Substituent Effects on the Photophysical Properties of Monobenzopentalenes

Downloaded from: https://research.chalmers.se, 2025-12-04 18:25 UTC

Citation for the original published paper (version of record):
Gazdag, T., Meiszter, E., Mayer, P. et al (2024). An Exploration of Substituent Effects on the Photophysical Properties of Monobenzopentalenes. ChemPhysChem, 25(7).
http://dx.doi.org/10.1002/cphc.202300737

N.B. When citing this work, cite the original published paper.

research.chalmers.se offers the possibility of retrieving research publications produced at Chalmers University of Technology. It covers all kind of research output: articles, dissertations, conference papers, reports etc. since 2004. research.chalmers.se is administrated and maintained by Chalmers Library

(article starts on next page)

Check for updates

ChemPhysChem

Research Article
doi.org/10.1002/cphc.202300737

Chemistry Europe
European Chemical Societies Publishing

www.chemphyschem.org

An Exploration of Substituent Effects on the Photophysical Properties of Monobenzopentalenes

Tamás Gazdag,[a, b] Enikő Meiszter,[a, c] Péter J. Mayer,[a, d] Tamás Holczbauer,[e] Henrik Ottosson,*[d] Andrew B. Maurer,*[f] Maria Abrahamsson,*[f] and Gábor London*[a]

Monobenzopentalenes have received moderate attention compared to dibenzopentalenes, yet their accessibility as stable, non-symmetric structures with diverse substituents could be interesting for materials applications, including molecular photonics. Recently, monobenzopentalene was considered computationally as a potential chromophore for singlet fission (SF) photovoltaics. To advance this compound class towards photonics applications, the excited state energetics must be characterized, computationally and experimentally. In this report we synthesized a series of stable substituted monobenzopentalenes and provided the first experimental exploration of their photophysical properties. Structural and optoelectronic characterization revealed that all derivatives showed ^{1}H NMR shifts in the olefinic region, bond length alternation in the pentalene unit, low-intensity absorptions reflecting the ground-state antiaromatic character and in turn the symmetry forbidden HOMO-to-LUMO transitions of ~2 eV and redox amphotericity. This was also supported by computed aromaticity indices (NICS, ACID, HOMA). Accordingly, substituents did not affect the fulfilment of the energetic criterion of SF, as the computed excited-state energy levels satisfied the required $E(S_1)/E(T_1) > 2$ relationship. Further spectroscopic measurements revealed a concentration dependent quenching of the excited state and population of the S_2 state on the nanosecond timescale, providing initial evidence for unusual photophysics and an alternative entry point for singlet fission with monobenzopentalenes.

Introduction

Molecular materials with embedded $4n\pi$-electron substructures with variously strong antiaromatic character have been explored recently as active components of molecular electronic devices.[1–15] The contribution of such subunits to decrease HOMO-LUMO gaps and promote redox amphoteric behavior underlies the vibrant research in the field.[16,17] Although in the majority of these applications antiaromatic scaffolds are used as organic semiconducting materials, their electronic features also allow for the control of excited state properties useful for molecular photonics including singlet fission (SF) photovoltaics[18] or photoredox processes.[19] These fields are currently dominated by small molecule aromatics, especially acene derivatives, however, materials with antiaromatic character[20,21] could form the basis of a new structural and functional chemical space in these areas. Yet, for the introduction of any new π-electron framework, the first step must be the exploration of the fundamental photophysical properties of its derivatives.

The key to the successful engineering of excited state properties is the ability to tune excited state energies such that desired photophysical processes are favored. Being able to tune singlet-triplet energy gaps is desirable for many applications, and especially so for SF photovoltaics. SF is a carrier multiplication process in which a singlet exciton (S_n) that is generated by the absorption of a photon, splits into two triplets (2 T_1).[18,22,23] For this to occur, the energy criterion of $E(S_1) > 2E(T_1)$ must be fulfilled. Tuning molecular properties towards efficient harnessing of singlet fission is foreseen to be the basis to significantly improve solar-energy conversion in

[a] T. Gazdag, E. Meiszter, P. J. Mayer, Dr. G. London
MTA TTK Lendület Functional Organic Materials Research Group, Institute of Organic Chemistry, HUN-REN Research Centre for Natural Sciences, 1117 Budapest, Magyar tudósok krt. 2, Hungary
E-mail: london.gabor@ttk.hu

[b] T. Gazdag
Hevesy György PhD School of Chemistry, Eötvös Loránd University, Pázmány Péter sétány 1/a, Budapest 1117, Hungary

[c] E. Meiszter
Department of Organic Chemistry and Technology, Faculty of Chemical Technology and Biotechnology, Budapest University of Technology and Economics, Műegyetem rkp. 3., H-1111 Budapest, Hungary

[d] P. J. Mayer, Prof. Dr. H. Ottosson
Department of Chemistry – Ångström Laboratory, Uppsala University, Box 523, Uppsala 751 20, Sweden
E-mail: henrik.ottosson@kemi.uu.se

[e] Dr. T. Holczbauer
Chemical Crystallography Research Laboratory and Stereochemistry Research Group, Institute for Organic Chemistry, HUN-REN Research Centre for Natural Sciences, 1117 Budapest, Magyar tudósok krt. 2, Hungary

[f] Dr. A. B. Maurer, Prof. Dr. M. Abrahamsson
Department of Chemistry and Chemical Engineering, Chalmers University of Technology, Gothenburg 41296, Sweden
E-mail: maurer@chalmers.se
abmaria@chalmers.se

Supporting information for this article is available on the WWW under https://doi.org/10.1002/cphc.202300737

© 2024 The Authors. ChemPhysChem published by Wiley-VCH GmbH. This is an open access article under the terms of the Creative Commons Attribution License, which permits use, distribution and reproduction in any medium, provided the original work is properly cited.

© 2024 The Authors. ChemPhysChem published by Wiley-VCH GmbH

photovoltaics.[24–26] Like in most organic electronics applications, acenes are considered key structures in realizing efficient singlet fission processes.[27–33] For the design of singlet fission chromophores beyond acenes[34] El Bakouri, Smith and Ottosson proposed a conceptual approach[35] based on the combined tuning of ground state Hückel-antiaromaticity/aromaticity and excited state Baird-aromaticity/antiaromaticity.[36–39] To identify new potential SF chromophores within a $4n\pi$-electron compound class they tuned the extent of ground state (S_0) antiaromaticity, whereby Baird-aromatic character and the energy levels of their lowest excited states, $E(S_1)$ and $E(T_1)$, could be tuned systematically.[35]

In the above mentioned computational analysis of potential singlet fission chromophores with ground state antiaromatic character, pentalene derivatives, primarily dibenzo[*a*,*f*]pentalene and monoarenopentalenes, were proposed to be suitable materials for this purpose.[35] Although both structures fulfill the energetic requirements for singlet fission ($E(S_1)/E(T_1) > 2$) dibenzo[*a*,*f*]pentalenes are difficult synthetic targets due to their low stability,[40,41] while stable monoarenopentalene derivatives are well-documented.[42–47] For the monobenzopentalene framework the calculated $E(S_1)/E(T_1)$ ratio was above the desired 2, however, $E(S_1) \approx E(T_2)$ was obtained[35] that could be a favorable energetic scenario for unwanted intersystem crossing, which interferes with the singlet fission process.[48] This latter suboptimal situation could potentially be overcome by the involvement of the $S_0 \rightarrow S_2$ excitation, which is optically allowed in pentalenes, in contrast to the symmetry-forbidden $S_0 \rightarrow S_1$ transition. As monobenzopentalene itself is unstable at ambient conditions,[49] its functionalization is necessary to access stable materials, which in turn may allow for further fine tuning of the energy levels. Furthermore, if the stability is high enough, with the energetic splitting designed with singlet fission in mind, emission from higher excited states is possible. Notably, singlet fission was demonstrated in a structurally somewhat related dibenzo[*a*,*e*]pentalene derivative,[50,51] however, that molecule with its two styryl substituents is likely better described as a 1,8-diphenyloctatetraene-type chromophore.[35]

The predictions from the Hückel/Baird SF chromophore design approach that monobenzopentalenes are expected to be suitable chromophores for singlet fission prompted us to systematically investigate computationally and experimentally the properties of a range of stable monobenzopentalene structures to address a few key questions. Which functional groups are tolerated by the synthetic methodology? Do these molecules with different functional groups as substituents satisfy the electronic criteria for SF? Is there a particular effect of the nature of the substituents (electron donor or acceptor) on the ground- and excited-state properties? Through an exploratory study of monobenzopentalene derivatives bearing electronically different substituents involving donor and acceptors groups or both in a readily available position, we aimed at answering these questions, which would provide the fundamental basis of the further development of this class of materials for molecular photonics applications in general and for SF photovoltaics in particular.

Results and Discussion

In the following, we first provide the synthesis and experimental characterization of a series of stable C6 substituted benzopentalenes, including ^{1}H NMR spectroscopy and X-ray crystallography. Next, we analyze the trends in their relevant energy levels with UV-vis spectroscopy, electrochemistry, photophysical investigations, and quantum chemical calculations. Towards the end, we explore by computational means how the position of the substitution impacts on the excited state energy levels.

Synthesis

For the synthesis of monobenzopentalenes (for detailed synthetic procedures see section S2, Supporting Information) we used the methodology based on the carbopalladation cascade between *gem*-dibromoolefins and acetylenes.[42] These compounds are characterized by better preserved antiaromaticity compared to dibenzo[*a*,*e*]pentalenes as they are stabilized only by a single fused benzene ring and three pendant phenyl groups. To facilitate the systematic comparison of a range of structures we chose to introduce substituents to the fused benzene ring at the C6 position, which has the most readily available starting materials (Figure 1). Twelve substituted monobenzopentalenes were prepared in moderate to good yields considering the formation of three new C–C bonds during the cascade reaction. Molecules with electron-donating and -withdrawing functional groups directly attached to the benzopentalene core (**3b**–**3f**) were synthesized, while substituents were also introduced to the pendant phenyl groups to probe potential donor-acceptor interactions within the molecules (**3g**, **3h**). Furthermore, structures that are extended with an acetylene spacer were also prepared (**3i**–**3m**). Notably, these acetylenic substituents (R^1) that were present in the starting dibromoolefins (**1**) were not involved in the cascade reaction showing that the intramolecular carbopalladation within **1** followed by the intermolecular reaction with the excess diarylacetylene reagent (**2**) is the dominating reaction pathway.[42,47] The unsubstituted derivative **3a** was used for comparison. Overall, most of the compounds were found to be stable, except for **3c** bearing the strongly donating dimethylamino substituent, which was found to decompose under ambient conditions. The nitro-group containing donor-acceptor substituted pentalene **3h** was found to degrade at aerobic conditions at elevated temperatures. Notably, by changing the nitro-group of **3h** to nitrile-group in **3g** led to increased stability.

The ^{1}H NMR chemical shifts of the protons attached to the pentalene cores were found below 6.5 ppm (500 MHz, CD_2Cl_2, 30 °C) for all compounds, consistent with antiaromatic character,[42–44,46,47] however, the actual values showed variation with the substituents on the fused benzene ring. The proton signal of compound **3a** with no substituents appeared at 6.35 ppm. Compared to **3a**, the proton signals of compounds with donor substituents shifted more upfield (**3b**, **3c**), while acceptor substituents (**3d**–**3f**) led to a relative downfield shift. The signals of the donor-acceptor systems **3g** and **3h** appeared

© 2024 The Authors. ChemPhysChem published by Wiley-VCH GmbH

14397641, 0, Downloaded from https://chemistry-europe.onlinelibrary.wiley.com/doi/10.1002/cphc.202300737 by Chalmers University Of Technology, Wiley Online Library on [01/03/2024]. See the Terms and Conditions (https://onlinelibrary.wiley.com/terms-and-conditions) on Wiley Online Library for rules of use; OA articles are governed by the applicable Creative Commons License

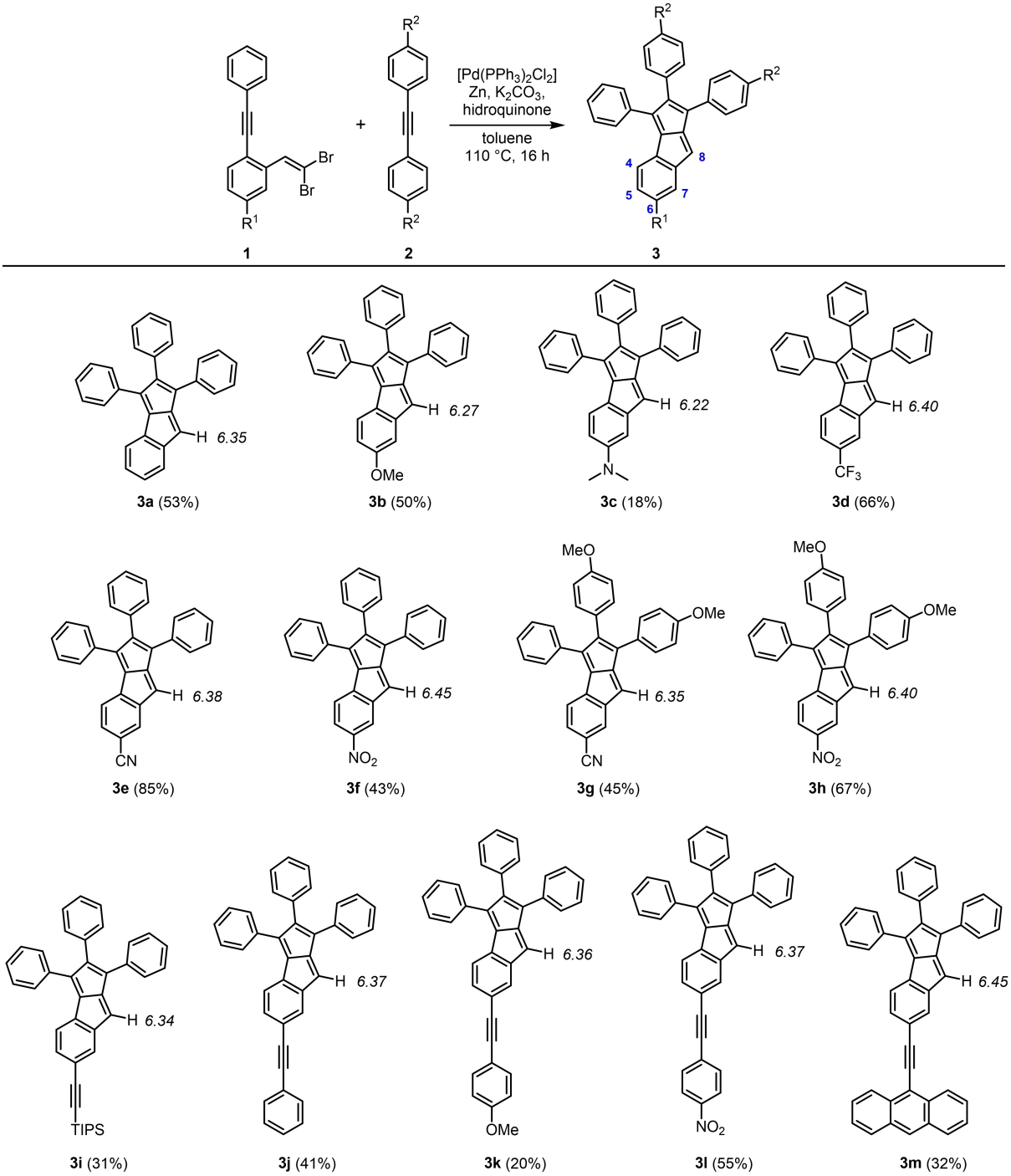

Figure 1. Monobenzopentalene derivatives synthesized for this study. The ^{1}H NMR shifts (500 MHz, CD_2Cl_2, 30 °C) of the pentalene protons are given in italics in ppm value (Isolated yields are given in parenthesis).

more upfield compared to the respective acceptor substituted compounds **3e** and **3f**, while comparably downfield relative to the compound containing only the methoxyphenyl substituents (compound **S35**, $\delta = 6.30$ ppm, Figure S1, Supporting Information). Functional groups within the alkynylated molecules **3i**–**3l** had little influence on the chemical shifts, except for the anthracene containing system **3m** where the pentalene proton shift was the same as for the nitro-group containing derivative **3f**.

A single crystal of compound **3m** suitable for X-ray diffraction measurement could be obtained (Figure 2) (for further details see section S3, Supporting Information). Considerable bond length alternation was found around the perimeter of the planar benzopentalene core that is characteristic to antiaromatic molecules, while the phenyl substituents were

© 2024 The Authors. ChemPhysChem published by Wiley-VCH GmbH

14397641, 0, Downloaded from https://chemistry-europe.onlinelibrary.wiley.com/doi/10.1002/cphc.202300737 by Chalmers University Of Technology, Wiley Online Library on [01/03/2024]. See the Terms and Conditions (https://onlinelibrary.wiley.com/terms-and-conditions) on Wiley Online Library for rules of use; OA articles are governed by the applicable Creative Commons License

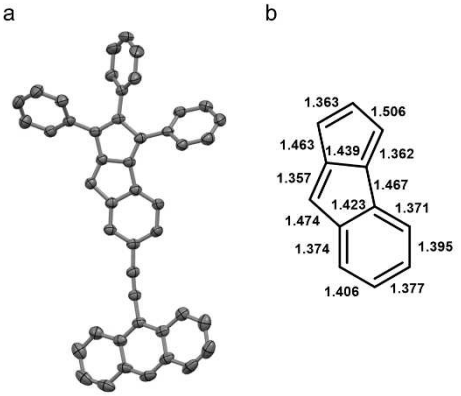

Figure 2. X-ray structure of **3 m** and the corresponding bond lengths (Å) (ORTEP style representation is drawn at the 50% probability level. Hydrogen atoms are omitted for clarity).

found non-coplanar, similarly as in previously reported related examples.[42–46]

Opto-electronic properties

The S_0-S_1 excitation energies for the prepared compounds were measured via UV-Vis spectroscopy, and also derived from cyclic voltammetry. The corresponding TD-DFT calculations were performed in a similar manner as utilized earlier (Table 1)[35] (for details on computations see section S5, Supporting Information). The UV-Vis spectra of the compounds that were directly substituted with donor or acceptor groups (**3 b**–**3 f**) showed little variation with the substituents (Figure 3a and Table 1). Notably, a bathochromic shift of the highest intensity absorption band was observed for the nitro-substituted compound **3 f**. Among the low-intensity, long-wavelength absorptions, which is characteristic to pentalenes due to their symmetry-forbidden HOMO-LUMO transitions, **3 c** with a dimethylamino substituent had a peak maximum at the highest wavelength (680 nm) within the whole series. Interestingly, the low-wavelength maxima were shifted bathochromically also in the case of the donor-acceptor substituted molecules **3 g** (λ_{max} = 649 nm) and **3 h** (λ_{max} = 670 nm) compared to the corresponding derivatives having only the acceptor substituents (**3 e**, λ_{max} = 613 nm; **3 f**, λ_{max} = 618 nm) (Figure 3b). Furthermore, the compound bearing only the 4-methoxyphenyl groups (**S35**) exhibited a maximum at 609 nm (Figure S1, Supporting Information), which is close to the maximum of **3 a** (λ_{max} = 600 nm). This suggests that although the pendant phenyl groups are not co-planar with the conjugated benzopentalene core, the joint presence of donor and acceptor groups affect the electronic structure of the molecules. For the acetylenic compounds **3 i**–**3 m** similar trends were observed as for the directly substituted compounds **3 b**–**3 f**, however, the molar absorption coefficients were generally higher due to the more extended π-systems (Figure 3c). This finding is also supported by the calculated oscillator strength for those molecules (Table S5, Supporting Information).

Cyclic voltammetry was used to evaluate the basic electrochemical properties of the prepared molecules (for further details see section S4, Supporting Information). The results are summarized in Table 1. Compound **3 c** was found to be unstable under the measurement conditions. Substituents within the series **3 b**–**3 f** led to a change in both the oxidation and reduction potentials compared to the unsubstituted compound **3 a**. The introduction of an electron-donating methoxy group (**3 b**) led to lower oxidation potential (0.48 V vs. 0.64 V for **3 a**), while the reduction potential somewhat increased (−1.61 V vs. −1.59 V for **3 a**). For the electron-withdrawing substituents the trend was the opposite with the largest changes in the case of the nitro-substituted molecule **3 f** (0.90 V, −1.22 V vs. 0.64 V, −1.59 V for **3 a**). Notably, the donor-acceptor substituted

Table 1. Summary of optical, electrochemical, and computation data on the HOMO, LUMO and S_0–S_1 transition.

Entry	Compound	λ_{abs1} [nm][a]	$E_{p,a,1}$ [V][b]	$E_{p,c,1}$ [V][b]	ΔE_{redox} [eV][c]	ΔE_{opt} [eV]	ΔE_{calc}[f] [eV]
1	**3 a**	600	0.64	−1.59	1.95	2.09	2.09
2	**3 b**	603	0.48[d]	−1.61	1.85	2.05	1.96
3	**3 c**	680	n.d.[e]	n.d.[e]	n.d.[e]	1.82	1.91
4	**3 d**	595	0.81	−1.39	1.92	2.08	2.10
5	**3 e**	613	0.79	−1.33	1.86	2.02	2.06
6	**3 f**	618	0.90	−1.22	1.8	2.01	2.06
7	**3 g**	649	0.59[d]	−1.38	1.71	1.91	1.98
8	**3 h**	670	0.65[d]	−1.26	1.63	1.85	1.97
9	**3 i**	614	0.65	−1.50	1.84	2.02	2.04
10	**3 j**	618	0.64	−1.50	1.83	2.01	2.02
11	**3 k**	618	0.66	−1.47	1.82	2.01	2.01
12	**3 l**	618	0.68	−1.37	1.79	2.01	2.02
13	**3 m**	618	0.61	−1.47	1.80	2.01	2.00

[a] Measured in $CHCl_3$ at rt. [b] Electrochemical measurements were carried out in 0.1 M Bu_4NPF_6 in dichloromethane at a scan rate of 0.1 $V s^{-1}$ on a glassy carbon working electrode. [c] Estimated from the differences between onset potentials. [d] Quasi-reversible first oxidation wave. [e] Compound **3 c** decomposed under the measurement conditions. [f] Calculated at the TD-M06-2X/def2-TZVPD//M06-2X/6-311+G(d,p) level.

© 2024 The Authors. ChemPhysChem published by Wiley-VCH GmbH

14397641, 0, Downloaded from https://chemistry-europe.onlinelibrary.wiley.com/doi/10.1002/cphc.202300737 by Chalmers University Of Technology, Wiley Online Library on [01/03/2024]. See the Terms and Conditions (https://onlinelibrary.wiley.com/terms-and-conditions) on Wiley Online Library for rules of use; OA articles are governed by the applicable Creative Commons License

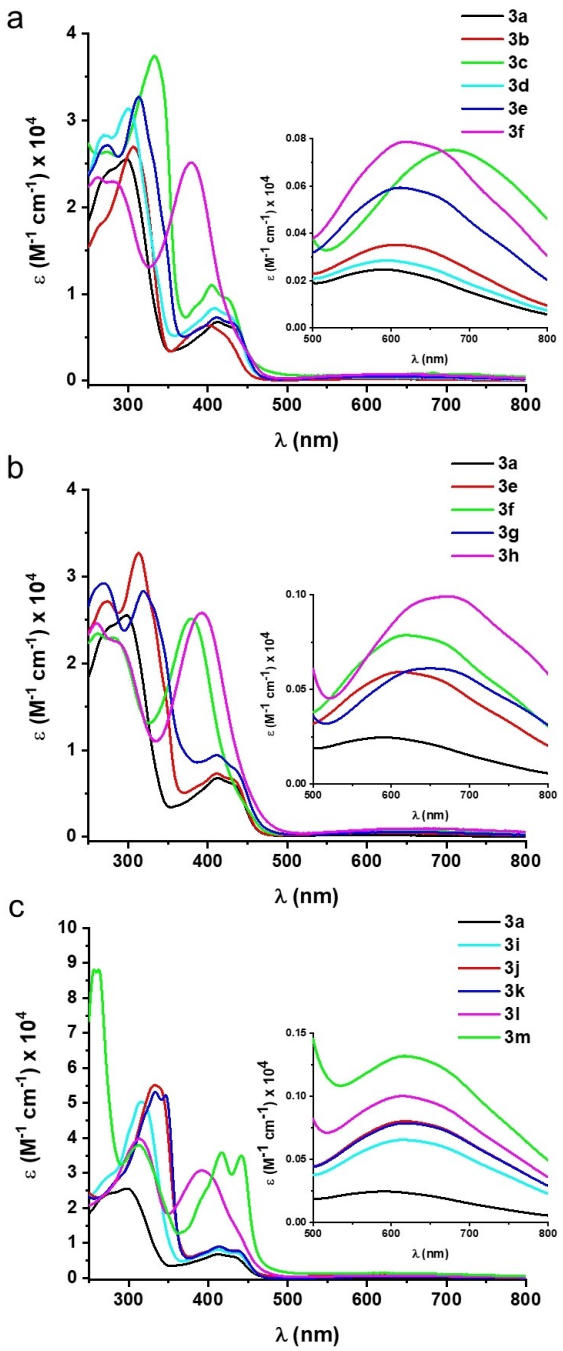

Figure 3. UV-Vis spectra of monobenzopentalenes **3a**–**3m** ($CHCl_3$, rt). (a) Spectra of directly substituted pentalenes **3b**–**3f**; (b) spectra of donor-acceptor substituted pentalenes **3g** and **3h** in comparison with the acceptor substituted molecules **3e** and **3f**; (c) spectra of acetylene containing pentalenes **3i**–**3m** (Spectrum of **3a** is used for comparison in all cases).

molecules **3g** and **3h** showed the highest redox-amphotericity as reflected in the smallest $\Delta E_{redox} = E_{on,a}$-$E_{on,c}$ values in their case (Table 1). Within the series of the acetylene-containing molecules the oxidation potentials were not strongly affected and found comparable to **3a** in each case, while the reduction potentials comparably decreased. In most cases the substituent-induced increase or decrease in the oxidation and reduction potentials changed in a concerted manner that did not strongly affect the HOMO-LUMO gaps. The electrochemically obtained HOMO-LUMO gaps, although following the same trend, were found consistently lower compared to the optical gap. The electrochemical gaps are rather approximative due to the irreversible electrochemical processes and the determination of the onset-potentials that were used for the calculation.

The HOMO-LUMO gaps for the molecules were also calculated at the TD–M06-2X/def2-TZVPD level, which performed best when the vertical excitation energies were compared to the UV-Vis spectra (for functional selection see section S5.2, in the Supporting Information),[52–54] This functional was also used in the earlier study by El Bakouri *et al.*[35] One can rationalize the small HOMO-LUMO gap by the ground and excited state (anti)aromatic nature of the substituted monobenzopentalanes as determined via the calculation of various aromaticity indices (section S5.4 in the Supporting Information).[55–59] Based on these indices, they showed significant ground state antiaromatic characters in line with the experimentally determined olefinic ^{1}H NMR chemical shifts, bond length alternation, and long wavelength, low intensity UV-vis spectral features. Notably, the level of antiaromaticity varied somewhat, however, it was not substantially affected by the nature of the substituent on the benzene ring.

Properties of the Excited States

Above we described the variation of the HOMO-LUMO gaps and the $S_0 \rightarrow S_1$ transition energies, yet, singlet fission, photoredox chemistry and many other molecular photonic phenomena rely also on other processes in the molecules. Below, we present results from computations and emission spectra of the monobenzopentalene derivatives.

From the singlet fission perspective the S_1, T_1, and T_2 excited states and their relative energies are important, however, for pentalene derivatives the inclusion of the S_2 state is also important since it has been shown that singlet fission occurs following $S_0 \rightarrow S_2$ excitation in a styryl-substituted dibenzopentalene derivative.[50] The energetic criteria ($2E(T_1) < E(S_1) < E(T_2)$) was evaluated within the prepared series of molecules with the computational scheme developed by Zeng, Hoffmann, and Ananth[60] and previously used by El Bakouri *et al.*[35] (see also section S5 in the Supporting Information). This approach uses adiabatic excitation to the T_1 state and vertical excitation to the S_1 and T_2 states from the optimized S_0 and T_1 structures, respectively. In addition, the vertical excitation to the S_2 state was included. During the evaluation, we also added data from ref. [35] on monobenzopentalene (**3a'**).

The data derived from the computations are visualized in Figure 4 (see also Table S5 in the Supporting Information). Overall, all synthesized structures fulfilled the basic energetic requirement regarding the relationship between $E(S_1)$ and $E(T_1)$. Furthermore, compared to the unsubstituted benzopentalene framework **3a'**,[35] where $E(S_1) \approx E(T_2)$, the introduction of the phenyl substituents, as in **3a**, increased the T_2 energy levels considerably above $E(S_1)$. The introduction of further substituents did not affect the $E(S_1) < E(T_2)$ arrangement, although the

© 2024 The Authors. ChemPhysChem published by Wiley-VCH GmbH

14397641, 0, Downloaded from https://chemistry-europe.onlinelibrary.wiley.com/doi/10.1002/cphc.202300737 by Chalmers University Of Technology, Wiley Online Library on [01/03/2024]. See the Terms and Conditions (https://onlinelibrary.wiley.com/terms-and-conditions) on Wiley Online Library for rules of use; OA articles are governed by the applicable Creative Commons License

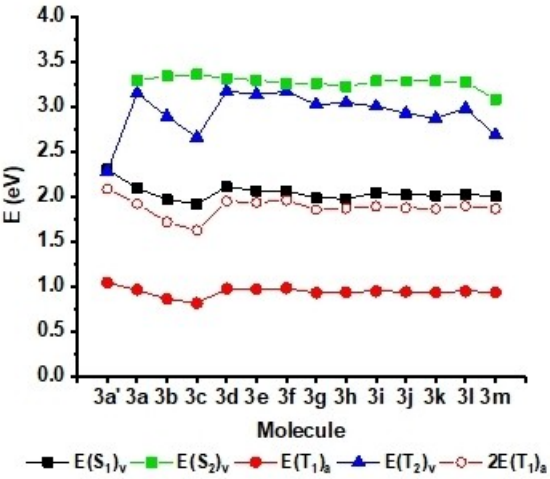

Figure 4. Variation of the calculated $E(S_1)_v$, $E(S_2)_v$, $E(T_1)_a$ and $E(T_2)_v$ within benzopentalenes **3a**–**3m**. $2E(T_1)_a$ is also shown to facilitate comparison with $E(S_1)_v$ and $E(T_2)_v$. **3a'** refers to the unsubstituted monobenzopentalene framework; data taken from ref. [35].

relative values varied slightly. These findings showed that $E(T_2)$ of benzopentalenes is affected more substantially by substituents than by increasing the size of the fused arene, a strategy that has been explored previously and led to various relationships between $E(S_1)$ and $E(T_2)$.[35] On the other hand, substituents affected $E(T_1)$ oppositely, because in all cases this energy decreased slightly when compared to the unsubstituted π-framework **3a'**. The relative tuning of $E(T_1)$ and $E(T_2)$ is crucial as $T_1 + T_1 \rightarrow T_2$ could be detrimental for harvesting SF-generated triplets unless $2E(T_1) < E(T_2)$ is fulfilled. Importantly, this latter requirement is satisfied by all substituted benzopentalene derivatives. Among the excited state energy levels studied $E(S_1)$, $E(T_1)$, and $E(T_2)$ were affected more by the presence of electron donating substituents (**3b**, **3c**), which decreased these energy values compared to the corresponding ones of **3a**, while electron withdrawing groups on the benzene rings had negligible effects. These differences reflect the extents of ground state antiaromatic character within the series. Specifically, **3b** and **3c** having electron donating groups are slightly more antiaromatic (S_0), which is also supported by various antiaromaticity indices (see section S5.4 in the Supporting Information). The substituents, however, influence $E(S_1)$ and $E(T_1)$ equally, as these energies change synchronously across the series. The $E(S_2)$ was consistent among the series, and the biggest difference was observed in **3m** which might be due to the anthracene subunit contribution to the transition from the S_0 state to the S_2 state (for further details see section S5.3 in the Supporting Information).

Next, we turn to the emissive properties of the molecules from the S_1 and S_2 states. The emission data presented was obtained in CH_3CN instead of $CHCl_3$ (which was used for the absorption measurements) due to increased quantum yield and in turn a better observed signal-to-noise ratio resulting in a more robust analysis. This solvent dependence points towards a polar excited state, as the more polar solvent stabilizes the molecule enough for emission. Small solvatochromism was observed due to the solvent polarity change, which is reflected in minor spectral shifts in different solvents (section S6, Supporting Information). Compound **3c** was not reported as it was found to be unstable under experimental conditions. Although potentially expected, due to the symmetry forbidden nature, relatively low energy gap, and low extinction coefficients of the HOMO-LUMO gap within these pentalenes, no discernible emission from the S_1 state could be identified. This could simply be due to weak emission coupled with the formally forbidden absorbance, rapid crossing into the triplet manifold, or other excited state processes such as singlet fission.

Interestingly, excitation at higher energies results in photoluminescence. Typically, as Kasha's rule would dictate, excitation at higher energy would result in rapid deactivation to the lowest excited state,[61,62] which here is non-emissive. The presence of emission at energies above the HOMO-LUMO gap provides an unusual property that is often sought after for molecular photonics,[63,64] particularly for OLEDs. This high-energy emission was influenced substantially by the substituents (Figure 5, Table 2).

Unlike the absorption profiles, the emission of the **3b**–**3f** compounds that were directly substituted with donor and acceptor groups showed large variations (Figure 5a). Compound **3b**, containing a π-electron donating methoxy group resulted in a hypsochromic shift ($\lambda_{max} = 435$ nm) in emission peak relative to **3a** ($\lambda_{max} = 448$ nm). The strong acceptor groups resulted in bathochromic shifts with the largest shift observed from **3e**. This shift was further increased in the donor-acceptor substituted molecules of **3g** ($\lambda_{max} = 512$ nm) and **3h** ($\lambda_{max} = 481$ nm) compared to their acceptor only derivatives (**3e**, $\lambda_{max} = 483$ nm; **3f**, $\lambda_{max} = 469$ nm) (Figure 5b). These results further confirm the hypothesis that the addition of substituents on the pendant phenyls, while not co-planar, directly effects the excited states. The acetylenic compounds add unusual complexities to the trends seen in **3b**–**3f**. Compounds **3i** and **3j** behave similarly to the absorption in that they are slightly bathochromically shifted. However, **3k** ($\lambda_{max} = 440$ nm) and **3l** ($\lambda_{max} = 434$ nm) have hypsochromic shifts that are relatively unaffected by the donating or withdrawing nature of the attached functional group. This hypsochromic shift is also observed in **3m** ($\lambda_{max} = 441$ nm). Furthermore, more vibrational character can be observed in all acetylenic species, with **3m** being the most pronounced. These trends point towards an alternative excited state being populated for the acetylenic compounds that has a higher degree of rigidity in the unit associated with the excited state.

Even with the symmetry-forbidden S_1, emission from a higher energy state is not particularly common. Indeed, the early reports of emission from an S_2 state come from azulene and azulene derivatives, in which the S_0-S_1 gap is of similar energy to the S_1-S_2 gap or the S_2 state can be thermally repopulated.[65] However, neither of these circumstances are applicable here and beyond that we see no S_1 emission. In fact, most examples of solution based S_2 emission results in emission from both the S_2 and S_1 and the S_1 is substantially higher in

© 2024 The Authors. ChemPhysChem published by Wiley-VCH GmbH

14397641, 0, Downloaded from https://chemistry-europe.onlinelibrary.wiley.com/doi/10.1002/cphc.202300737 by Chalmers University Of Technology, Wiley Online Library on [01/03/2024]. See the Terms and Conditions (https://onlinelibrary.wiley.com/terms-and-conditions) on Wiley Online Library for rules of use; OA articles are governed by the applicable Creative Commons License

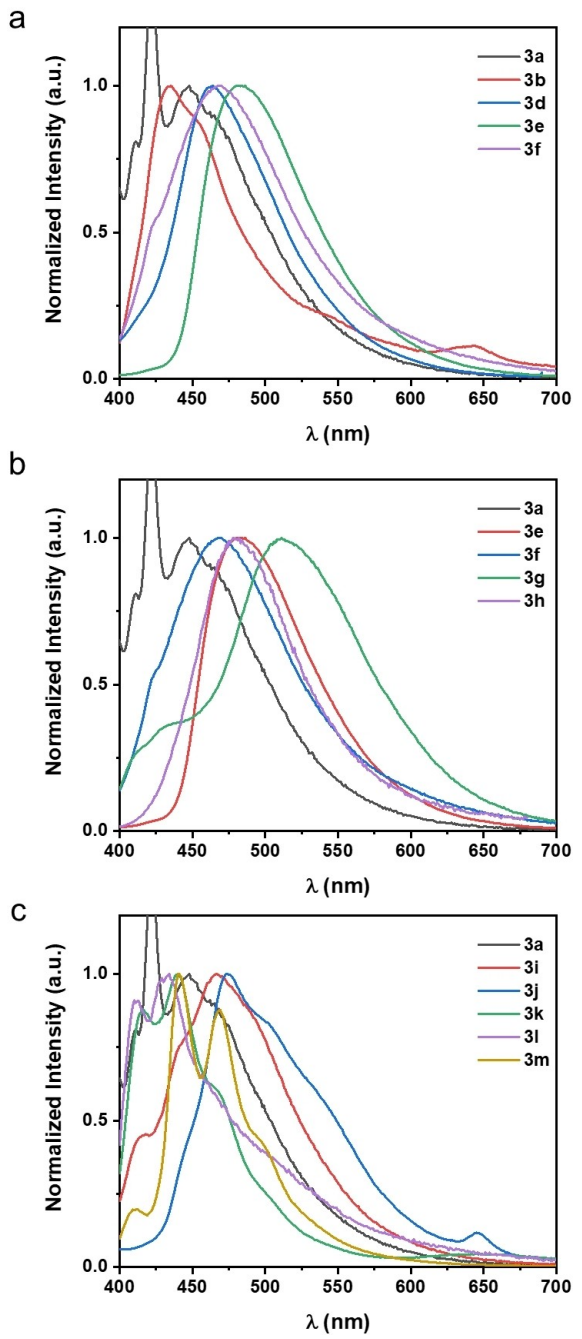

Figure 5. Normalized steady-state emission spectra of monobenzopentalenes **3a**–**3m** (CH_3CN, λ_{ex}: 377 nm, rt, air). (a) Spectra of directly substituted pentalenes **3b**–**3f**; (b) spectra of donor-acceptor substituted pentalenes **3g** and **3h** in comparison with the acceptor substituted molecules **3e** and **3f**; (c) spectra of acetylene containing pentalenes **3i**–**3m** (Note that the spectrum of **3a** which is used for comparison in all cases also show Raman scattering from the solvent).

emissive intensity with few notable exceptions. For thiones and triphenylmethane dyes, the S_1 absorption band also has a weak extinction coefficient. However, the S_2 state has an emission rate that is competitive with internal conversion, or relaxation process, with fluorescence lifetimes on the order of <1 ns.[66–68] This allows strong emission from the S_2 state due to reduced relaxation. The compounds presented here do not have emission rates on that timescale, however, this explanation could be possible if the internal conversion was slow enough. Notably, the cause of the anti-Kasha behavior among azulenes was recently described in terms of excited state (anti)aromaticity.[69]

One important clue to identify what is happening is that the emission quantum yields are estimated to be <1%. While low emission yields may suggest impurities, beyond synthetic purity confirmation, the observed trends across the series of compounds synthesized follow expected interactions with the substituents, the emission shifts mimic S_2 absorbance shifts, and the excitation spectra follow the UV-vis spectra reasonably well. This means that most of the generated excited-states undergo the anticipated non-radiative relaxation pathways. In fact, with quantum yields and lifetimes of this magnitude, the non-radiative rate constants are on the order of 10^8 s^{-1}, rates on the same order of magnitude of previously reported $S_2 \rightarrow S_1$ internal conversion rates of magnesium porphyrin complexes with similar $E(S_2)$-$E(S_1)$ energy gap of ~8000 cm^{-1}.[70] The appearance of the S_2 emission can be attributed in part to slowed non-radiative pathways but also to the lack of any overbearing S_1 emission. While the explanation may be as straightforward as strong oscillator strength and slow internal conversion due to a large energy gap, further investigation into this emissive S_2 state is warranted.

Outside of the unusual excited-state mechanics, lifetimes were also taken in diffuse conditions to determine if the excited states were long-lived enough to interact for singlet fission. Time-correlated single photon counting results used to determine lifetime are included in the Supporting Information (section S6). As shown in Table 2, the lifetimes of the compounds varied but all were on the ns timescale. Similar trends to the observed results in steady state emission spectra demonstrate a longer lifetime for the donating group in **3b** ($\tau=$ 8.4 ns), and the shortest lifetime for **3e** ($\tau=3.2$ ns). Unlike those steady state trends, the donor-acceptor compounds saw a large change for **3g** ($\tau=10.3$ ns) while from **3f** ($\tau=5.2$ ns) to **3h** ($\tau=$ 5.3 ns) almost no noticeable change is observed. The acetylenic compounds had much shorter lifetimes on average, supporting the steady state results that seem to indicate a change in excited state nature.

Several compounds, **3a**, **3b**, **3f**, **3i**, and **3k** provided unusual results as they showed non-mono-exponential decay dynamics. It was found that the <1 ns decay for **3a**, **3b**, and **3f** was only present in $CHCl_3$ and not in CH_3CN, providing a possible explanation for why the quantum yield in CH_3CN was substantially higher. While this warrants further investigation, the breadth of this paper does not allow for in-depth analysis into sub-nanosecond timescale mechanisms. Compounds **3i** and **3k** also have this unusual feature, however, the rate can be resolved. This may be indicative of a different decay pathway; the "short" lifetime present is on the order of the longer timescale for most other species and is the dominant decay. At this time both lifetimes are reported, and the assumption is held that the dominant lifetime is representative of fluorescence from the S_2 state. Provided high concentrations or increased intermolecular interaction, lifetimes observed here

© 2024 The Authors. ChemPhysChem published by Wiley-VCH GmbH

14397641, 0, Downloaded from https://chemistry-europe.onlinelibrary.wiley.com/doi/10.1002/cphc.202300737 by Chalmers University Of Technology, Wiley Online Library on [01/03/2024]. See the Terms and Conditions (https://onlinelibrary.wiley.com/terms-and-conditions) on Wiley Online Library for rules of use; OA articles are governed by the applicable Creative Commons License

Table 2. Summary of emissive data.

Entry	Compound	λ_{abs2} [nm][a]	λ_{em1} [nm][b]	τ [ns][b]	QY (%)[f]	k_f ($\times 10^3$ s^{-1})[f]	$k_{n.r.}$ ($\times 10^8$ s^{-1})[f]	$E(S_2)_v$[g] [eV]
1	**3a**	413	448	4.7	0.12	255	2.1	3.29
2	**3b**	401	435	8.6	0.16	186	1.2	3.33
3	**3c**	405	n.d[c]	n.d[c]	n.d[c]	n.d[c]	n.d[c]	3.35
4	**3d**	412	463	3.8	0.02	52.6	2.6	3.31
5	**3e**	414	483	3.2	0.03	93.8	3.1	3.29
6	**3f**	379	469	5.2	0.003	5.77	1.9	3.25
7	**3g**	411	512	10.3	0.08	77.7	1.0	3.26
8	**3h**	392	481	5.3	0.003	5.67	1.9	3.22
9	**3i**	411	467	2.6, 16.6[d]	0.06	231[d]	3.9	3.28
10	**3j**	414	479	2.4	0.11	458	4.2	3.28
11	**3k**	414	440	2.6, 33.2[d]	0.04	154[d]	3.9	3.28
12	**3l**	391	434	<1[e]	0.004[f]	40.0[e]	0.1[e]	3.27
13	**3m**	438	441	3.5	0.01	28.6	2.9	3.08

[a] Measured in $CHCl_3$ at rt. [b] Measured in CH_3CN at rt with 377 nm excitation. [c] Compound **3c** decomposed under the measurement conditions. [d] Non-first-order decay. [e] Lifetime was less than observable with a ns laser diode. [f] See SI for details on calculation. [g] Calculated at the TD-M06-2X/def2-TZVPD//M06-2X/6-311+G(d,p) level.

would suffice for singlet fission or other photoreactions to occur should they be allowed.

Typically, in solution-based singlet fission experiments, high concentrations are utilized to encourage the chance of an excited state interacting with a ground state molecule.[28] To check on the possibility of singlet fission or any photoreactivity, the singlet lifetime was monitored with increasing concentrations[28,71] It was found that increasing the concentration of the monobenzopentalene reduced the lifetime of the excited state, from 8.6 ns to 3.4 ns, a clear indication of excited state photoreactivity (Figure 6). It should be noted however that quenching via singlet fission typically occurs when varying concentration on significantly higher scales (mM), and as such the degree of quenching is likely either supplemented by another process or enhanced due to the larger driving forces present from interaction with the S_2 state. Ultrafast transient absorption experiments can be utilized to ensure whether the quenching of this excited state is due to singlet fission or some other process, however, this kind of ultrafast analysis is beyond the scope of this work.

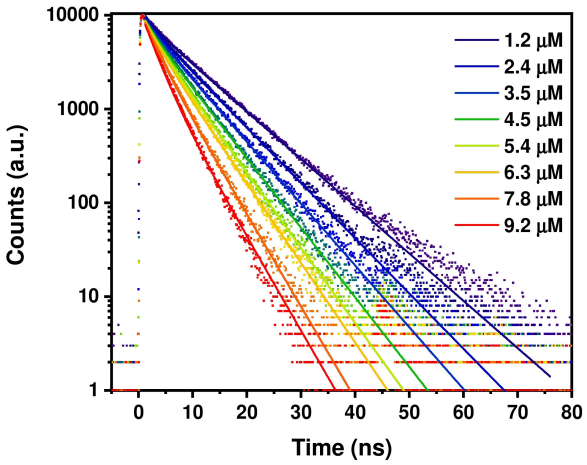

Figure 6. Time-correlated single photon counting (TCSPC) lifetime measurements of **3b** in CH_3CN following excitation with a 377 nm pulsed laser diode at increasing concentrations.

Expanded analysis of substituent effects

We found that even with diverse substituents at the C6 position of the benzene ring, the photo-physical properties of the molecules were affected only to a minor extent (Table 1, Figure 4). The largest differences were observed in their emission properties from the S_2 states (Table 2). As the substitution pattern used in this study was guided by synthetic accessibility, it is instructive to compute alternative patterns that might have a greater impact on energetics and hence could be interesting further synthetic targets. For such predictions we calculated the excited state properties of molecules having electron donor or acceptor groups in different positions along the monobenzopentalene framework (Figure 7). Furthermore, as functional groups directly attached to the pentalene unit could strongly impact molecular properties, as exemplified recently for 1,3-bis(dimethylamino)pentalene,[72] we studied the effect of substituents on the available pentalene C–H position in benzopentalene.

Independent of the position of the substituents, the basic criteria for SF is theoretically satisfied by all molecules (Figure 7). The energetics of the T_1, S_1, and T_2 states depended modestly on the substituent position along the benzene ring. This could be due to excited state aromaticity in monobenzopentalene moieties (for further details see section S5.4 in the Supporting Information) whereby the substituents affect the delocalization only to a minor extent. However, it is interesting that in **3b5**

© 2024 The Authors. ChemPhysChem published by Wiley-VCH GmbH

14397641, 0, Downloaded from https://chemistry-europe.onlinelibrary.wiley.com/doi/10.1002/cphc.202300737 by Chalmers University Of Technology, Wiley Online Library on [01/03/2024]. See the Terms and Conditions (https://onlinelibrary.wiley.com/terms-and-conditions) on Wiley Online Library for rules of use; OA articles are governed by the applicable Creative Commons License

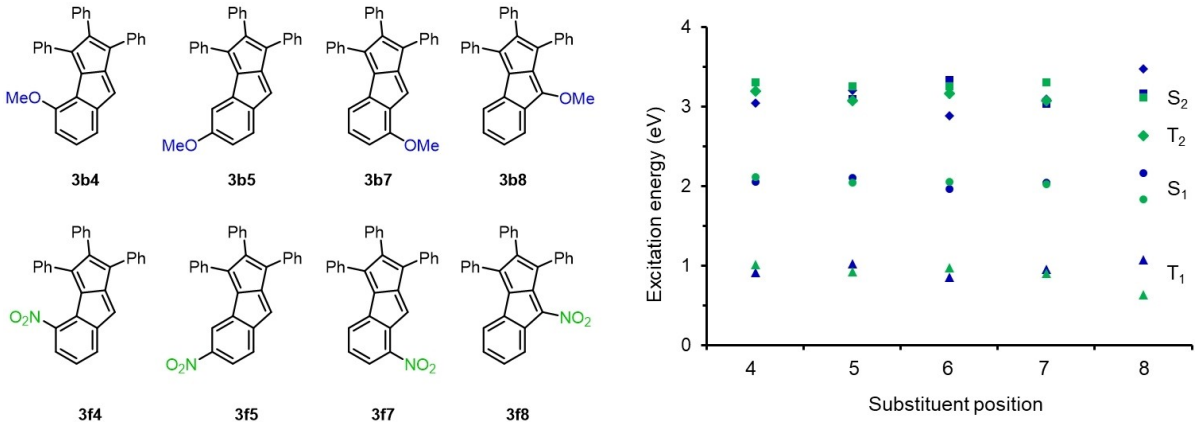

Figure 7. Substituent effects on energetics in monobenzopentalene derivatives with methoxy and nitro groups at different positions. Triangles correspond to adiabatic T_1 energies. Circles, squares, and diamonds correspond to the energies of the vertical excitation to the S_1, S_2, and T_2 states, respectively.

and **3 b7** the order of the energetics changes so that $E(T_2) > E(S_2)$, which could be of use in the future. The largest substituent effects were obtained upon direct substitution of the pentalene unit. The $E(T_1)$ of the methoxy substituted molecule (**3 b8**) is around 1.1 eV, which is desirable as it is close the band gap of silicon.[73] However, we must note that although these compounds have interesting properties based on the calculations for their preparation, the development of a new synthetic methodology is necessary.

Conclusions

A novel set of monobenzopentalenes have been synthesized and characterized. The synthetic methodology tolerated a wide range of functional groups on the C6 position of the benzene ring including donor and acceptor substituents providing access to electronically tuned structures.

Computational efforts indicated an energetic possibility of singlet fission with expected S_1 energy levels being greater than or equal to twice the T_1 energy levels for all synthesized molecules, independent of their functional groups. Beyond that the T_2 states are too high in energy to be accessed from unwanted processes. Ground state absorption and electrochemistry measurements helped to confirm the expected trends and values obtained through computational work.

Hence, these monobenzopentalenes provide a new possible molecular set for applications in singlet fission photovoltaics, where electronically different substituents do not disturb the energetics. This feature will facilitate the tuning of monobenzopentalenes for solution processability and solid-state assembly, which are important in device applications, through substitution without the risk of affecting the energetic criteria of SF.

Regarding their photophysical properties, spectroscopic measurements revealed that while no emissive S_1 state was observed, the S_2 state could be populated and emit. This unusual feature is attributed in part to the symmetry-forbidden electronic nature of the S_1 state that likely also prevents strong emission from the S_1 state if it were to be populated. Excited-state lifetimes were also determined to be between <1 and 33.2 ns for the S_2 state, timeframes that could allow for singlet fission to occur in concentrated solution.

Expanded computation analysis on the effect of the functional group position around the benzopentalene framework revealed that SF criteria is satisfied independent of the position and electronic nature of the substituents. This further strengthens the advantage of this scaffold in SF photovoltaics applications through its structural tunability for *e.g.* environmental stability, solubility, solid-state assembly, while keeping the energetic criteria essentially unaffected.

Overall, these novel monobenzopentalenes provide a unique opportunity to advance molecular photonics and as such sub-nanosecond studies are due to be performed. Early indications of concentration dependent reduction of lifetime suggest excited state photoreactivity indicative of intermolecular interactions needed in both photoredox catalysis and singlet fission.

Experimental Section

General Information

Commercial reagents, solvents and catalysts (Aldrich, Fluorochem, VWR) were purchased as reagent–grade and used without further purification. Solvents for extraction or column chromatography were of technical quality. For spectroscopy and sample treatment opti-grade quality solvents were used. Organic solutions were concentrated by rotary evaporation at 25–40 °C. Thin layer chromatography was carried out on SiO_2-layered aluminium plates (60778-25EA, Fluka). Column chromatography was performed using SiO_2-60 (230–400 mesh ASTM, 0.040–0.063 mm from Merck) at 25 °C or using a Teledyne Isco CombiFlash® Rf+ automated flash chromatographer with silica gel (25–40 μm, Redisep Gold®). Room temperature refers to 25–20 °C depending on the time of day.

NMR spectra were acquired on a Varian 500 NMR spectrometer, running at 500 and 126 MHz for ^{1}H and ^{13}C. The residual solvent peaks were used as the internal reference. Chemical shifts (δ) are reported in ppm. The following abbreviations are used to indicate the multiplicity in ^{1}H NMR spectra: s, singlet; d, doublet; t, triplet; q,

© 2024 The Authors. ChemPhysChem published by Wiley-VCH GmbH

14397641, 0, Downloaded from https://chemistry-europe.onlinelibrary.wiley.com/doi/10.1002/cphc.202300737 by Chalmers University Of Technology, Wiley Online Library on [01/03/2024]. See the Terms and Conditions (https://onlinelibrary.wiley.com/terms-and-conditions) on Wiley Online Library for rules of use; OA articles are governed by the applicable Creative Commons License

quartet; p, pentett; m, multiplet. ^{13}C NMR spectra were acquired on a broad band decoupled mode.

UV-Vis spectrophotometry was executed on a Jasco V-750 or a Perkin-Elmer Lambda 465 spectrophotometer. Hellma Analytics High Precision quartz cuvettes were used with optical path length of 1.0 cm.

Steady State Emission spectra were collected on a Fluorolog at a right angle using a R928 Hamamatsu detector.

Time-resolved single photon counting measurements were performed in a LifeSpec II collection apparatus, using a pulsed laser diode, picoquant II, whose repetition rate was adjusted based on the measured lifetime to ensure the system returned to equilibrium after pulse.

General Procedure for the Carbopalladation Cascade Reaction

Dibromoolefin (0.22 mmol, 1 eq), diphenylacetylene (200 mg, 1.10 mmol, 5 eq), K_2CO_3 (61 mg, 0.44 mmol, 2 eq), $Pd(PPh_3)_2Cl_2$ (16 mg, 10 mol% Pd), Zn powder (20 mg, 0.3 mmol, 1.4 eq) and dry toluene (4 mL) was stirred in a sealed vial under inert atmosphere (N_2) for 1 h at 110 °C in an aluminum heating block. The reaction was cooled to room temperature, and subsequently hydroquinone (30 mg, 0.27 mmol, 1.2 eq) was added to the reaction mixture and it was stirred at 110 °C for additional 16 h. After the reaction was completed, the mixture was diluted with EtOAc and washed with water (2×) and brine (1×). The organic phase was dried over $MgSO_4$. The solvent was evaporated under reduced pressure and the products was purified by column chromatography (SiO_2, *n*-hexane→*n*-hexane/EtOAc (12:1)).

Supporting Information

The authors have cited additional references within the Supporting Information (Ref. [74–94]).

Acknowledgements

Financial support from the Lendület Program of the Hungarian Academy of Sciences and the National Research, Development and Innovation Office, Hungary (NKFIH Grant FK 142622 (G.L.)) is gratefully acknowledged. G.L. acknowledges the János Bolyai Research Scholarship from the Hungarian Academy of Sciences. We are grateful to Krisztina Németh (MS Metabolomics Research Group, Instrumentation Center, HUN-REN TTK) for HRMS measurements. The Carl Trygger Foundation for a postdoctoral scholarship to P.M. (grant CTS 22:2330) and the Swedish Research Council for financial support to H.O. (grant 2019-05618) are gratefully acknowledged. The computations were enabled by resources provided by the National Academic Infrastructure for Supercomputing in Sweden (NAISS) and the Swedish National Infrastructure for Computing (SNIC) at the National Supercomputer Center (NSC) Linköping, partially funded by the Swedish Research Council through grant agreements no. 2022-06725 and no. 2018-05973.

Conflict of Interests

The authors declare no conflict of interest.

Data Availability Statement

The data that support the findings of this study are available in the supplementary material of this article.

Keywords: antiaromaticity · excited state · pentalene · photophysics · singlet fission · substituent effects

[1] T. Kawase, T. Fujiwara, C. Kitamura, A. Konishi, Y. Hirao, K. Matsumoto, H. Kurata, T. Kubo, S. Shinamura, H. Mori, E. Miyazaki, K. Takimiya, *Angew. Chem. Int. Ed.* **2010**, *49*, 7728–7732.
[2] M. Nakano, I. Osaka, K. Takimiya, *J. Mater. Chem. C* **2015**, *3*, 283–290.
[3] C. Liu, S. Xu, W. Zhu, X. Zhu, W. Hu, Z. Li, Z. Wang, *Chem. Eur. J.* **2015**, *21*, 17016–17022.
[4] G. Dai, J. Chang, W. Zhang, S. Bai, K.-W. Huang, J. Xu, C. Chi, *Chem. Commun.* **2015**, *51*, 503–506.
[5] C. Li, C. Liu, Y. Li, X. Zhua, Z. Wang, *Chem. Commun.* **2015**, *51*, 693–696.
[6] G. Dai, J. Chang, L. Jing, C. Chi, *J. Mater. Chem. C* **2016**, *4*, 8758–8764.
[7] J. Wilbuer, D. C. Grenz, G. Schnakenburg, B. Esser, *Org. Chem. Front.* **2017**, *4*, 658–663.
[8] J. L. Marshall, K. Uchida, C. K. Frederickson, C. Schutt, A. M. Zeidell, K. P. Goetz, T. W. Finn, K. Jarolimek, L. N. Zakharov, C. Risko, R. Herges, O. D. Jurchescud, M. M. Haley, *Chem. Sci.* **2016**, *7*, 5547–5558.
[9] Z. Zhang, H. Fana, X. Zhu, *Org. Chem. Front.* **2017**, *4*, 711–716.
[10] S. Yang, M. Chua, Q. Miao, *J. Mater. Chem. C* **2018**, *6*, 3651–3657.
[11] A. M. Zeidell, L. Jennings, C. K. Frederickson, Q. Ai, J. J. Dressler, L. N. Zakharov, C. Risko, M. M. Haley, O. D. Jurchescu, *Chem. Mater.* **2019**, *31*, 6962–6970.
[12] J. Wang, M. Chu, J.-X. Fan, T.-K. Lau, A.-M. Ren, X. Lu, Q. Miao, *J. Am. Chem. Soc.* **2019**, *141*, 3589–3596.
[13] Z. Jin, Z.-F. Yao, K. P. Barker, J. Pei, Y. Xia, *Angew. Chem. Int. Ed.* **2019**, *58*, 2034–2039.
[14] M. Gao, H. Chen, Q. Miao, *Eur. J. Org. Chem.* **2022**, *2022*, e202101315.
[15] K. Horii, A. Nogata, Y. Mizuno, H. Iwasa, M. Suzuki, K.-i. Nakayama, A. Konishi, M. Yasuda, *Chem. Lett.* **2022**, *51*, 325–329.
[16] R. Breslow, *Acc. Chem. Res.* **1973**, *6*, 393–398.
[17] T. M. Krygowski, M. K. Cyrański, Z. Czarnocki, G. Häfelinger, A. R. Katritzky, *Tetrahedron* **2000**, *56*, 1783–1796.
[18] M. B. Smith, J. Michl, *Chem. Rev.* **2010**, *110*, 6891–6936.
[19] N. A. Romero, D. A. Nicewicz, *Chem. Rev.* **2016**, *116*, 10075–10166.
[20] A. Konishi, M. Yasuda, *Chem. Lett.* **2021**, *50*, 195–212.
[21] C. Hong, J. Baltazar, J. D. Tovar, *Eur. J. Org. Chem.* **2022**, *2022*, e202101343.
[22] M. B. Smith, J. Michl, *Annu. Rev. Phys. Chem.* **2013**, *64*, 361–386.
[23] D. Casanova, *Chem. Rev.* **2018**, *118*, 7164–7207.
[24] J. Lee, P. Jadhav, P. D. Reusswig, S. R. Yost, N. J. Thompson, D. N. Congreve, E. Hontz, T. Van Voorhis, M. A. Baldo, *Acc. Chem. Res.* **2013**, *46*, 1300–1311.
[25] A. Rao, R. H. Friend *Nature Rev. Mater.* **2017**, *2*, 17063.
[26] R. Casillas, I. Papadopoulos, T. Ullrich, D. Thiel, A. Kunzmann, D. M. Guldi, *Energy Environ. Sci.* **2020**, *13*, 2741–2804.
[27] S. T. Roberts, R. E. McAnally, J. N. Mastron, D. H. Webber, M. T. Whited, R. L. Brutchey, M. E. Thompson, S. E. Bradforth, *J. Am. Chem. Soc.* **2012**, *134*, 6388–6400.
[28] B. J. Walker, A. J. Musser, D. Beljonne, R. H. Friend, *Nat. Chem.* **2013**, *5*,1019–1024.
[29] D. N. Congreve, J. Lee, N. J. Thompson, E. Hontz, S. R. Yost, P. D. Reusswig, M. E. Bahlke, S. Reineke, T. Van Voorhis, M. A. Baldo, *Science* **2013**, *340*, 334–337.
[30] A. Kunzmann, M. Gruber, R. Casillas, J. Zirzlmeier, M. Stanzel, W. Peukert, R. R. Tykwinski, D. M. Guldi, *Angew. Chem. Int. Ed.* **2018**, *57*, 10742–10747.
[31] M. Einzinger, T. Wu, J. F. Kompalla, H. L. Smith, C. F. Perkinson, L. Nienhaus, S. Wieghold, D. N. Congreve, A. Kahn, M. G. Bawendi, M. A. Baldo, *Nature* **2019**, *571*, 90–94.

© 2024 The Authors. ChemPhysChem published by Wiley-VCH GmbH

14397641, 0, Downloaded from https://chemistry-europe.onlinelibrary.wiley.com/doi/10.1002/cphc.202300737 by Chalmers University Of Technology, Wiley Online Library on [01/03/2024]. See the Terms and Conditions (https://onlinelibrary.wiley.com/terms-and-conditions) on Wiley Online Library for rules of use; OA articles are governed by the applicable Creative Commons License

[32] B. S. Basel, I. Papadopoulos, D. Thiel, R. Casillas, J. Zirzlmeier, T. Clark, D. M. Guldi, R. R. Tykwinski, *Trends Chem.* **2019**, *1*, 11–21.
[33] T. Hasobe, S. Nakamura, N. V. Tkachenko, Y. Kobori, *ACS Energy Lett.* **2022**, *7*, 390–400.
[34] T. Ullrich, D. Munz, D. M. Guldi, *Chem. Soc. Rev.* **2021**, *50*, 3485–3518.
[35] O. El Bakouri, J. R. Smith, H. Ottosson, *J. Am. Chem. Soc.* **2020**, *142*, 5602–5617.
[36] N. C. Baird, *J. Am. Chem. Soc.* **1972**, *94*, 4941–4948.
[37] H. Ottosson, *Nat. Chem.* **2012**, *4*, 969–971.
[38] M. Rosenberg, C. Dahlstrand, K. Kilså, H. Ottosson, *Chem. Rev.* **2014**, *114*, 5379–5425.
[39] L. J. Karas, I. J. Wu, *Nat. Chem.* **2022**, *14*, 723–725.
[40] A. Konishi, Y. Okada, M. Nakano, K. Sugisaki, K. Sato, T. Takui, M. Yasuda, *J. Am. Chem. Soc.* **2017**, *139*, 15284–15287.
[41] A. Konishi, Y. Okada, R. Kishi, M. Nakano, M. Yasuda, *J. Am. Chem. Soc.* **2019**, *141*, 560–571.
[42] P. Rivera-Fuentes, M. von Wantoch Rekowski, W. B. Schweizer, J.-P. Gisselbrecht, C. Boudon, F. Diederich, *Org. Lett.* **2012**, *14*, 4066–4069.
[43] G. London, M. von Wantoch Rekowski, O. Dumele, W. B. Schweizer, J.-P. Gisselbrecht, C. Boudon, F. Diederich, *Chem. Sci.* **2014**, *5*, 965–972.
[44] J. Cao, G. London, O. Dumele, M. von Wantoch Rekowski, N. Trapp, L. Ruhlmann, C. Boudon, A. Stanger, F. Diederich, *J. Am. Chem. Soc.* **2015**, *137*, 7178–7188.
[45] S.-i. Kato, S. Kuwako, N. Takahashi, T. Kijima, Y. Nakamura, *J. Org. Chem.* **2016**, *81*, 7700–7710.
[46] T. Gazdag, P. J. Mayer, P. P. Kalapos, T. Holczbauer, O. El Bakouri, G. London, *ACS Omega* **2022**, *7*, 8336–8349.
[47] P. J. Mayer, G. London, *Org. Lett.* **2023**, *25*, 42–46.
[48] A. Japahuge, T. Zeng, *ChemPlusChem* **2018**, *83*, 146–182.
[49] R. F. C. Brown, N. Choi, K. J. Coulston, F. W. Eastwood, U. E. Wiersum, L. W. Jenneskens, *Tetrahedron Lett.* **1994**, *35*, 4405–4408.
[50] Y. Wu, Y. Wang, J. Chen, G. Zhang, J. Yao, D. Zhang, H. Fu, *Angew. Chem. Int. Ed.* **2017**, *56*, 9400–9404.
[51] L. Wang, Y. Wu, Y. Liu, L. Wang, J. Yao, H. Fu, *J. Chem. Phys.* **2019**, *151*, 124701.
[52] Gaussian 16, Revision C.01, M. J. Frisch, G. W. Trucks, H. B. Schlegel, G. E. Scuseria, M. A. Robb, J. R. Cheeseman, G. Scalmani, V. Barone, G. A. Petersson, H. Nakatsuji, X. Li, M. Caricato, A. V. Marenich, J. Bloino, B. G. Janesko, R. Gomperts, B. Mennucci, H. P. Hratchian, J. V. Ortiz, A. F. Izmaylov, J. L. Sonnenberg, D. Williams-Young, F. Ding, F. Lipparini, F. Egidi, J. Goings, B. Peng, A. Petrone, T. Henderson, D. Ranasinghe, V. G. Zakrzewski, J. Gao, N. Rega, G. Zheng, W. Liang, M. Hada, M. Ehara, K. Toyota, R. Fukuda, J. Hasegawa, M. Ishida, T. Nakajima, Y. Honda, O. Kitao, H. Nakai, T. Vreven, K. Throssell, J. A. Montgomery Jr., J. E. Peralta, F. Ogliaro, M. J. Bearpark, J. J. Heyd, E. N. Brothers, K. N. Kudin, V. N. Staroverov, T. A. Keith, R. Kobayashi, J. Normand, K. Raghavachari, A. P. Rendell, J. C. Burant, S. S. Iyengar, J. Tomasi, M. Cossi, J. M. Millam, M. Klene, C. Adamo, R. Cammi, J. W. Ochterski, R. L. Martin, K. Morokuma, O. Farkas, J. B. Foresman, D. J. Fox, Gaussian, Inc., Wallingford CT, 2016.
[53] Y. Zhao, D. G. Truhlar, *Theor. Chem. Acc.* **2008**, *120*, 215–241.
[54] F. Weigend, *Phys. Chem. Chem. Phys.* **2006**, *8*, 1057–1065.
[55] J. Kruszewski, T. M. Krygowski, *Tetrahedron Lett.* **1972**, *13*, 3839–3842.
[56] D. Geuenich, K. Hess, F. Köhler, R. Herges, *Chem. Rev.* **2005**, *105*, 3758–3772.
[57] R. Gershoni-Poranne, A. Stanger, *Chem. Eur. J.* **2014**, *20*, 5673–5688.
[58] P. Bultinck, R. Ponec, S. Van Damme, *J. Phys. Org. Chem.* **2005**, *18*, 706–718.
[59] E. Matito, M. Duran, M. Solà, *J. Chem. Phys.* **2005**, *122*, 014109.
[60] T. Zeng, R. Hoffmann, N. Ananth, *J. Am. Chem. Soc.* **2014**, *136*, 5755–5764.
[61] M. Kasha, *Discuss. Faraday Soc.* **1950**, *9*, 14–19.
[62] S. E. Braslavsky, *Pure Appl. Chem.* **2007**, *79*, 293–465.
[63] K. Veys, D. Escudero, *Acc. Chem. Res.* **2022**, *55*, 2698–2707.
[64] R. P. Steer, *Phys. Chem. Chem. Phys.* **2023**, *25*, 23384–23394.
[65] M. Beer, H. C. Longuet-Higgins, *J. Chem. Phys.* **1955**, *23*, 1390–1391.
[66] M. H. Hui, P. de Mayo, R. Suau, W. R. Ware, *Chem. Phys. Lett.* **1975**, *31*, 257–263.
[67] A. Maciejewski, *Chem. Phys. Lett.* **1989**, *164*, 166–172.
[68] P. Singhal, H. N. Ghosh, *Phys. Chem. Chem. Phys.* **2014**, *16*, 16824–16831.
[69] D. Dunlop, L. Ludvíková, A. Banerjee, H. Ottosson, T. Slanina, *J. Am. Chem. Soc.* **2023**, *145*, 21569–21575.
[70] R. R. Valiev, R. T. Nasibullin, V. N. Cherepanov, A. Kurtsevich, D Sundholm, T. Kurtén, *Phys. Chem. Chem. Phys.* **2021**, *23*, 6344–6348.
[71] M. Dvořák, S. K. K. Prasad, C. B. Dover, C. R. Forest, A. Kaleem, R. W. MacQueen, A. J. Petty II, R. Forecast, J. E. Beves, J. E. Anthony, M. J. Y. Tayebjee, A. Widmer-Cooper, P. Thordarson, T. W. Schmidt, *J. Am. Chem. Soc.* **2021**, *143*, 13749–13758.
[72] V. Thery, C. Barra, A. Simeoni, J. Pecaut, E. Tomas-Mendivil, D. Martin, *Org. Lett.* **2023**, *25*, 560–564.
[73] T. C. Wu, N. J. Thompson, D. N. Congreve, E. Hontz, S. R. Yost, T. Van Voorhis, M. A. Baldo, *Appl. Phys. Lett.* **2014**, *104*, 193901.
[74] T. Yamada, K. Park, T. Tachikawa, A. Fujii, M. Rudolph, A. S. K. Hashmi, H. Sajiki, *Org. Lett.* **2020**, *22*, 1883–1888.
[75] A. Gandini, M. Bartolini, D. Tedesco, L. Martinez-Gonzalez, C. Roca, N. E. Campillo, J. Zaldivar-Diez, C. Perez, G. Zuccheri, A. Miti, A. Feoli, S. Castellano, S. Petralla, B. Monti, M. Rossi, F. Moda, G. Legname, A. Martinez, M. L. Bolognesi, *J. Med. Chem.* **2018**, *61*, 7640–7656.
[76] M.-S. Tsai, C.-L. Ou, C.-J. Tsai, Y.-C. Huang, Y.-C. Cheng, S.-S. Sun, J.-S. Yang, *J. Org. Chem.* **2017**, *82*, 8031–8039.
[77] A. A. Mikhaylov, A. D. Dilman, R. A. Novikov, Y. A. Khoroshutina, M. I. Struchkova, D. E. Arkhipov, Y. V. Nelyubina, A. A. Tabolin, S. L. Ioffe, *Tetrahedron Lett.* **2016**, *57*, 11–14.
[78] CrystalClear SM 1.4.0 Rigaku/MSC Inc., **2008**.
[79] NUMABS: T. Higashi, (1998), rev. **2002**. (Rigaku/MSC Inc.) .
[80] G. M. Sheldrick, *Acta Crystallogr.* **2008**, *A64*, 112–122.
[81] G. M. Sheldrick, *Acta Crystallogr.* **2015**, *C71*, 3–8.
[82] L. J. Farrugia, *J. Appl. Crystallogr.* **2012**, *45*, 849–854.
[83] A. L. Spek, *Acta Crystallogr.* **2009**, *D65*, 148–155.
[84] O. V. Dolomanov, L. J. Bourhis, R. J. Gildea, J. A. K. Howard, H. Puschmann, *J. Appl. Crystallogr.* **2009**, *42*, 339–341.
[85] C. F. Macrae, P. R. Edgington, P. McCabe, E. Pidcock, G. P. Shields, R. Taylor, M. Towler, J. van de Streek, *J. Appl. Crystallogr.* **2006**, *39*, 453–457.
[86] R. Krishnan, J. S. Binkley, R. Seeger, J. A. Pople, *J. Chem. Phys.* **1980**, *72*, 650–654.
[87] K. Jorner, F. Feixas, R. Ayub, R. Lindh, M. Solà, H. Ottosson, *Chem. Eur. J.* **2016**, *22*, 2793–2800.
[88] T. Lu, F. Chen, *J. Comput. Chem.* **2012**, *33*, 580–592.
[89] R. Herges, ACID software package https://www.otto-diels-institut.de/herges/pages_en/projects_acid.html.
[90] A. Stanger, A. Rahalkar, Aroma, https://chemistry.technion.ac.il/en/team/amnon-stanger/.
[91] E. Matito, ESI-3D: Electron Sharing Indexes Program for 3D Molecular Space Partitioning, Institute of Computational Chemistry and Catalysis, Girona, Catalonia, Spain, **2006**, https://ematito.webs.com/programs.htm.
[92] AIMAll (Version 17.11.14 B) TK Gristmill Software (aim.tkgristmill.com), Overland Park KS, USA, **2018**.
[93] A data set collection of computational results is available in the ioChem-BD repository and can be accessed via https://doi.org/10.19061/iochem-bd-6-290; M. Ivarez-Moreno, C. de Graaf, N. Lopez, F. Maseras, J. M. Poblet, C. J. Bo, *J. Chem. Inf. Model.* **2015**, *55*, 95–103.
[94] R. Grotjahn, T. M. Maier, J. Mitch, M. Kaupp, *J. Chem. Theory Comput.* **2017**, *13*, 4984–4996.

Manuscript received: October 9, 2023
Revised manuscript received: December 18, 2023
Accepted manuscript online: January 29, 2024
Version of record online: ■■, ■■

© 2024 The Authors. ChemPhysChem published by Wiley-VCH GmbH

14397641, 0, Downloaded from https://chemistry-europe.onlinelibrary.wiley.com/doi/10.1002/cphc.202300737 by Chalmers University Of Technology, Wiley Online Library on [01/03/2024]. See the Terms and Conditions (https://onlinelibrary.wiley.com/terms-and-conditions) on Wiley Online Library for rules of use; OA articles are governed by the applicable Creative Commons License

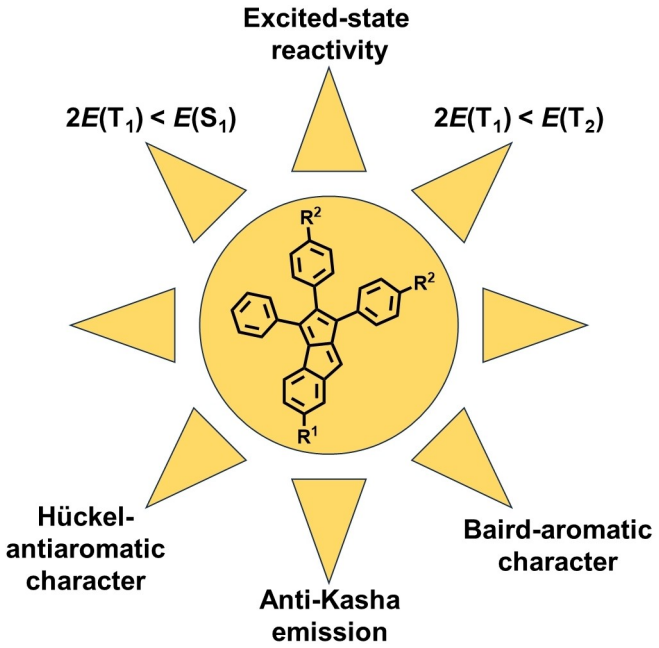

A novel set of monobenzopentalenes have been synthesized and characterized that could provide an opportunity to advance molecular photonics and in particular the field of singlet fission.

T. Gazdag, E. Meiszter, P. J. Mayer, Dr. T. Holczbauer, Prof. Dr. H. Ottosson, Dr. A. B. Maurer*, Prof. Dr. M. Abrahamsson*, Dr. G. London**

1 – 12

An Exploration of Substituent Effects on the Photophysical Properties of Monobenzopentalenes

14397641, 0, Downloaded from https://chemistry-europe.onlinelibrary.wiley.com/doi/10.1002/cphc.202300737 by Chalmers University Of Technology, Wiley Online Library on [01/03/2024]. See the Terms and Conditions (https://onlinelibrary.wiley.com/terms-and-conditions) on Wiley Online Library for rules of use; OA articles are governed by the applicable Creative Commons License